VERSITA

Central European Journal of Physics
DOI: 10.2478/s11534-007-0016-7
Research article
CEJP 5(3) 2007 293–312

Computational studies of steady-state sound field and reverberant sound decay in a system of two coupled rooms

Mirosław Meissner*

Institute of Fundamental Technological Research,
Polish Academy of Sciences,
PL-00–049 Warsaw, Poland

Received 16 November 2006; accepted 7 March 2007

Abstract: The acoustical properties of an irregularly shaped room consisting of two connected rectangular subrooms were studied. An eigenmode method supported by a numerical implementation has been used to predict acoustic characteristics of the coupled system, such as the distribution of the sound pressure in steady-state and the reverberation time. In the theoretical model a low-frequency limit was considered. In this case the eigenmodes are lightly damped, thus they were approximated by normal acoustic modes of a hard-walled room. The eigenfunctions and eigenfrequencies were computed numerically via application of a forced oscillator method with a finite difference algorithm. The influence of coupling between subrooms on acoustic parameters of the enclosure was demonstrated in numerical simulations where different distributions of absorbing materials on the walls of the subrooms and various positions of the sound source were assumed. Calculation results have shown that for large differences in the absorption coefficient in the subrooms the effect of modal localization contributes to peaks of RMS pressure in steady-state and a large increase in the reverberation time.

Keywords: Coupled rooms, modal analysis, reverberation time, modes localization
PACS (2006): 43.20.+g, 43.55.+p

1 Introduction

Room acoustics is the study of the transient and steady-state behaviour of sound waves in enclosures. Various theories exist for predicting the acoustic parameters of rooms:

* E-mail: mmeissn@ippt.gov.pl

geometrical theory [1], wave theory [2], ray-tracing techniques, and statistical or power flow methods [3]. Geometrical room acoustics at best applies to highly reverberant rooms whose characteristic dimensions are large compared to the wavelength. This theory passes over diffraction phenomena since propagation in straight lines is its main postulate. Likewise, interference of sound waves is not considered.

Wave theory is the most reliable and appropriate from the physical point of view and is therefore essential for the understanding of sound propagation in enclosures. An immediate practical application of wave theory is limited to low frequencies in which the room dimensions are usually comparable with the sound wavelength. In this theory the response of a room can be understood in terms of its normal modes and the associated decay constant of each of these modes [4]. As was shown by Dowell [5], for weakly damped rooms the coupling between modes may be neglected and the distribution of mode amplitudes can be well described by eigenfunctions for rigid room walls. Closed form solutions of the wave equation can only be obtained for the simplest room shapes such rectangular, triangular and cylindrical ones. An application of the wave theory to complex enclosure geometries such as coupled rooms was possible through numerical methods. Examples of coupled enclosures are theatres with boxes which communicate with a main room through small apertures only, or churches with several naves and chapels.

The acoustic properties of coupled rooms have been investigated intensively in the past. Acoustic coupling between two rooms has been studied both theoretically and experimentally by Eyring [6]. Harris and Feshbach [7] have applied wave theory to the problem of acoustically coupled rooms and found explanations of some discrepancies noted by earlier researchers between an experiment and predictions from geometrical acoustics. The energy flux between two rooms has been investigated in detail by Cremer and Müller [8] for cases in which the rooms are coupled to an open area and when they are coupled through a door or window. They found that the strongest coupling occurs when one of the two rooms contains a large amount of acoustic absorption and the second room is more reverberant. Thomson [9] examined the acoustic wave propagation in coupled spaces and obtained an approximate solution for the pressure using the method of matched asymptotic expansions. Weaver and Lobkis [10] have showed theoretically and experimentally that the energy flow in weakly coupled reverberant systems can be Anderson localized. The acoustics of large buildings divided by arches and columns into coupled rooms has been examined by Anderson *et al.* [11, 12] to predict the decay of the sound energy density and the reverberation time. They reported a non-exponential decay of sound in different locations of coupled room systems such as St Paul's Cathedral in London [12] and investigated in particular the early decay of a sound that contributes mostly to its subjective perception. The effect of three architectural parameters: the ratio of the volume between the main and secondary rooms, the ratio between the rooms' absorption, and the size of a coupling aperture on the non-exponential decay of sound in a system of two connected rooms has been studied by Bradley and Wang [13]. They proposed a new objective method of quantifying the double-sloped effect (DSE) and

carried out tests to determine the subjective response to the DSE. In recent works several numerical methods such as ray-tracing techniques [14], statistical methods [15], and a method based on a diffusion model [16] were used to predict the decay of sound in systems of coupled rooms.

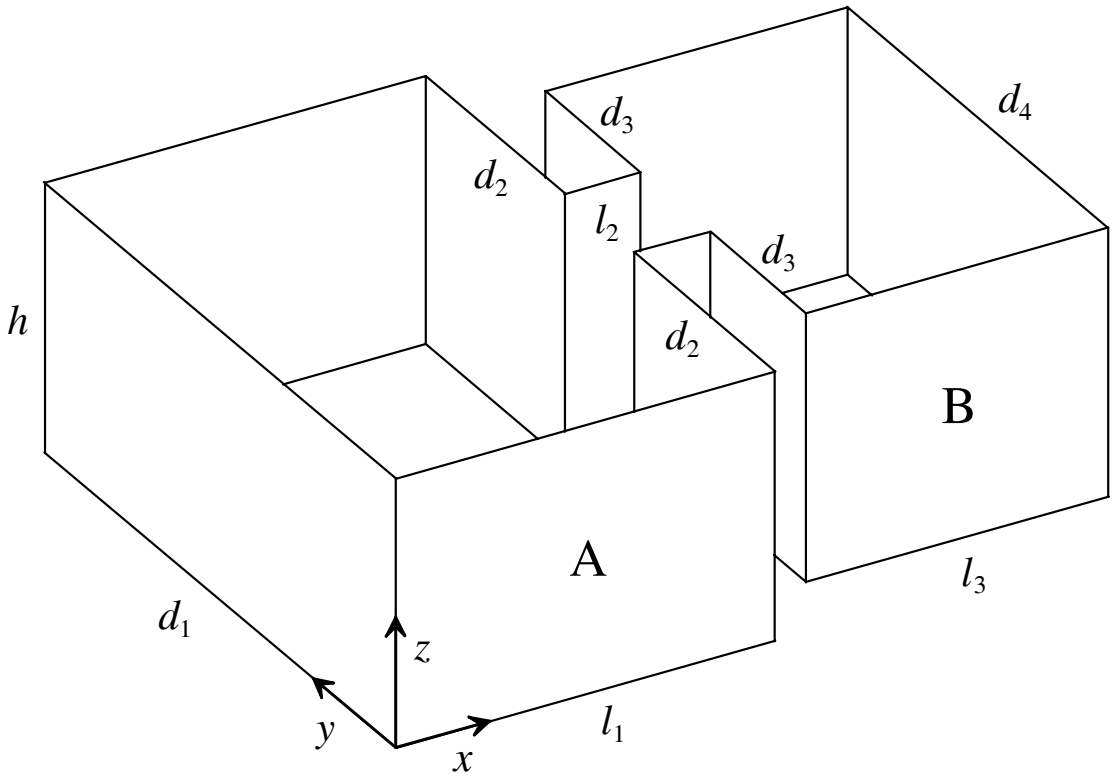

Fig. 1 Analysed room consisting of two connected rectangular subrooms denoted by A and B.

The present paper has been dedicated to computational studies of the steady-state and reverberant sound fields in a room consisting of two connected rectangular subrooms (Fig. 1). The room dimensions were assumed to be comparable with the sound wavelength, therefore a combination of a classical modal analysis with a numerical implementation was used in predicting the distribution of sound pressure inside the room and the pressure level decay curves. The room was considered as a weakly damped system so coupling terms in the solution of the wave equation were neglected and the pressure variable was expanded in normal modes for which the boundary conditions are rigid walls. To obtain better understanding of the acoustics in coupled spaces the steady-state and reverberant behaviour of the sound field were investigated for different distributions of absorbing materials under the condition that the total room absorption remained constant. Calculation results have shown that for large differences of sound damping in the subrooms the acoustic pressure distribution and the reverberation time are strongly influenced by the phenomenon of eigenmode localization.

2 Theory

In the low frequency limit a theoretical description of the acoustic field inside an irregularly shaped room is based on a solution of the wave equation with specified initial and boundary conditions [4]. From this point of view the room may be treated as a resonator with characteristic acoustic normal modes determined by the eigenfunctions $\Phi_{mn}(\mathbf{r}), \mathbf{r} = (x, y, z)$, and the eigenfrequencies ω_{mn}, $m = 0, 1, 2...$ and $n = 0, 1, 2...$, which depend on the boundary conditions and the room geometry. The functions Φ_{mn} are mutually orthogonal and it is assumed that they are normalized in the volume V of the room. In this case the formula for the acoustic pressure p has the form

$$p(\mathbf{r}, t) = \sqrt{V} \sum_{m=0}^{\infty} \sum_{n=0}^{\infty} P_{mn}(t)\, \Phi_{mn}(\mathbf{r}), \tag{1}$$

where the functions P_{mn} determine the steady-state behavior of the pressure of a room in time when it is excited by a sound source, or describe the process of acoustic pressure decay when the source is switched off. The eigenfunctions Φ_{mn} are mutually coupled through the impedance condition on absorptive walls

$$\frac{\partial p}{\partial n} = -\frac{\rho}{Z} \frac{\partial p}{\partial t}, \tag{2}$$

where $\partial/\partial n$ is a derivative taken in a direction normal to the surface S of the room's walls. However, in the range of low frequencies, where typical materials are characterized by a low absorption: $\Re\mathrm{e}(Z/\rho c) \ll 1$, where Z is the wall impedance, ρ is the density of air and c is the sound speed, it is possible to assume that the distribution of the mode amplitudes is well approximated by uncoupled eigenfunctions computed for perfectly rigid room walls [5]. For the enclosure shown in Fig. 1 the normalized eigenfunctions can be determined by

$$\Phi_{mn}(x, y, z) = \begin{cases} 1/\sqrt{V}, & m = 0,\ n = 0, \\ \Psi_n(x, y)/\sqrt{h}, & m = 0,\ n > 0, \\ \sqrt{2/h}\cos(m\pi z/h)\, \Psi_n(x, y), & m > 0,\ n > 0, \end{cases} \tag{3}$$

where h is the room height and the eigenfunctions Ψ_n are normalized over a horizontal cross-section of the room. In this case the eigenfrequencies are given by

$$\omega_{mn} = \sqrt{\left(\frac{m\pi c}{h}\right)^2 + \omega_n^2}, \tag{4}$$

where the frequencies ω_n satisfy the following two-dimensional eigenvalue equation

$$\nabla^2 \Psi_n + \left(\frac{\omega_n}{c}\right)^2 \Psi_n = 0. \tag{5}$$

Analytic forms of the eigenfunctions Ψ_n have been known for rooms with the simplest geometry only, like a rectangular prism or a cylinder. For irregularly shaped enclosures

finite element methods [17, 18], boundary element methods [19], and a variety of numerical implementations such as the forced oscillator method [20], a method based on the correspondence between the wave equation and the diffusion equation [21, 22] and a method of point-matching [23] have been applied to find the forms of eigenfunctions.

Assume that a source term in the wave equation has the form $-Q(\mathbf{r})\cos(\omega t)$, where $Q(\mathbf{r})$ and ω are the volume source distribution and the sound frequency, and the acoustic pressure $p(\mathbf{r}, t)$ satisfies homogeneous initial conditions and the boundary condition (2). In this case the function describing time behaviour of the first mode $(m, n = 0)$, the so-called Helmholtz mode that has an eigenfrequency equal to zero, is described by [24]

$$P_{00}(t) = \frac{Q_{00}\exp(-2r_{00}t)}{\omega^2 + 4r_{00}^2} + \frac{Q_{00}\cos(\omega t - \gamma_{00})}{\omega\sqrt{\omega^2 + 4r_{00}^2}}, \tag{6}$$

where $Q_{00} = \frac{c^2}{V}\int_V Q(\mathbf{r})\,\mathrm{d}v$ is a factor determining a source strength for the Helmholtz mode, $r_{00} = \frac{\rho c^2}{2V}\int_S Z^{-1}\,\mathrm{d}s$ is a damping coefficient and $\gamma_{00} = -\tan^{-1}(2r_{00}/\omega)$. As may be seen, the time component of the pressure for the Helmholtz mode consists of two parts: a transient term which disappears time increases and a steady-state harmonic term with a frequency ω equal to that of the sound source. The sum of these terms describes a process of a sound build-up in a room. For all other modes the formula for functions P_{mn} is given by [24]

$$P_{mn}(t) = -\frac{Q_{mn}\exp(-r_{mn}t)\,\omega_{mn}\cos(\Omega_{mn}t - \beta_{mn})}{\Omega_{mn}\sqrt{(\omega_{mn}^2 - \omega^2)^2 + 4r_{mn}^2\omega^2}} + \frac{Q_{mn}\cos(\omega t - \gamma_{mn})}{\sqrt{(\omega_{mn}^2 - \omega^2)^2 + 4r_{mn}^2\omega^2}}, \tag{7}$$

where $Q_{mn} = \frac{c^2}{\sqrt{V}}\int_V Q(\mathbf{r})\,\Phi_{mn}(\mathbf{r})\,\mathrm{d}v$ is a factor determining the source strength for the mode (m, n) and $r_{mn} = \frac{\rho c^2}{2}\int_S \Phi_{mn}^2(\mathbf{r})/Z\,\mathrm{d}s$ is a the modal damping coefficient. In Eq. (7) the quantity $\Omega_{mn} = \sqrt{\omega_{mn}^2 - r_{mn}^2}$ is the eigenfrequency for oscillations with damping, sometimes called the damped eigenfrequency [25], and β_{mn} and γ_{mn} are phase shifts given by

$$\beta_{mn} = \tan^{-1}\left[\frac{r_{mn}(\omega_{mn}^2 + \omega^2)}{\Omega_{mn}(\omega_{mn}^2 - \omega^2)}\right], \qquad \gamma_{mn} = \tan^{-1}\left[\frac{2r_{mn}\omega}{\omega_{mn}^2 - \omega^2}\right]. \tag{8a,b}$$

As follows from Eq. (7), for modes (m, n) with non-zero eigenfrequencies the time component of the pressure includes a transient harmonic term having the frequency Ω_m. Inserting Eqs. (6) and (7) into Eq. (1) enables prediction of the transient acoustic response of a room subjected to a harmonic source and more importantly, the acoustic pressure in steady-state. After simple transformations one may obtain a formula for the root mean square value of this pressure and the result is

$$P(\mathbf{r}) = \sqrt{\frac{V}{2}\sum_{m=0}^{\infty}\sum_{n=0}^{\infty}\frac{Q_{mn}^2\,\Phi_{mn}^2(\mathbf{r})}{(\omega_{mn}^2 - \omega^2)^2 + 4r_{mn}^2\omega^2}}, \tag{9}$$

showing that for a given room geometry the spatial distribution of RMS pressure depends on the driving frequency ω and, through the parameters Q_{mn}, on the volume source distribution $Q(\mathbf{r})$.

When a signal driving a room is switched off, the acoustic energy accumulated inside the room is dissipated on the walls and a reverberation, due to the common decay of eigenmodes, occurs. The time components of the pressure describing a process of sound decay in a room are determined by [26]

$$P_{00}(t) = -\frac{Q_{00}\exp(-2r_{00}t)}{\omega^2 + 4r_{00}^2}, \quad P_{mn}(t) = \frac{Q_{mn}\exp(-r_{mn}t)\,\omega_{mn}\cos(\Omega_{mn}t - \beta_{mn})}{\Omega_{mn}\sqrt{(\omega_{mn}^2 - \omega^2)^2 + 4r_{mn}^2\omega^2}}, \tag{10a,b}$$

and as may be seen, the components P_{00} and P_{mn} in the case of a sound decay and the transient terms in Eqs. (6) and (7) taken with opposite sign are identical. Inserting expressions (10a,b) into Eq. (1) leads to a formula for a reverberant sound field.

3 Analysis

3.1 Modal response

In a computational study the following room dimensions were assumed (in meters): $l_1 = 5$, $l_2 = 1$, $l_3 = 4$, $d_1 = 8$, $d_2 = 3.2$, $d_3 = 2.2$, $d_4 = 6$, $h = 3$ (Fig. 1), which seem to be typical dimensions for small flats. For this room configuration the unknown eigenfunctions Ψ_n and eigenfrequencies ω_n in Eqs. (3) and (4) were calculated numerically by the use of the program EIGEN, which was written in the Pascal language. In this program the forced oscillator method [20] with a finite difference algorithm was applied.

The forced oscillator method is based on the principle that a response of linear system to a periodic excitation is large when the driving frequency is close to the frequency of an eigenmode. In this method the eigenvalue problem is solved with the use of the analytical solution of the inhomogeneous wave equation in two space dimensions

$$c^2\nabla^2 f - \frac{\partial^2 f}{\partial t^2} = -q(x,y)\cos(\omega t), \tag{11}$$

where $q(x,y)$ determines the source distribution, which satisfies the Neumann boundary condition and the homogeneous initial conditions

$$f(x,y,t=0) = (\partial f/\partial t)_{t=0} = 0. \tag{12}$$

A numerical form of this solution is the following

$$f(i,j,k\tau) = \sum_{n=0}^{\infty} \frac{Q_n\,\Psi_n(i,j)[\cos(\omega_n k\tau) - \cos(\omega k\tau)]}{\omega^2 - \omega_n^2}, \tag{13}$$

where (i,j) is a grid point, τ is the time step, $k = 1, 2, 3, ..., K$, and

$$Q_n = \int_\sigma q(x,y)\Psi_n(x,y)\,\mathrm{d}x\mathrm{d}y, \tag{14}$$

where σ is a surface of the room's horizontal cross-section. Now, if the driving frequency ω is close to the eigenfrequency ω_n, then for sufficiently large time $\mathcal{T} = \tau K$ only the term connected with the mode number n contributes to the sum in Eq. (13), so one can write

$$f(i, j, \mathcal{T}) \approx a\,\Psi_n(i, j), \tag{15}$$

where a is a constant. The spatial distribution of Ψ_n can be determined after a normalization procedure which results in the elimination of the constant. Finally, use of the formula

$$\omega_n = c\sqrt{-\int_\sigma \Psi_n \nabla^2 \Psi_n \,\mathrm{d}i\,\mathrm{d}j} \tag{16}$$

found directly from Eq. (5) enables calculation of the eigenfrequency ω_n.

Using the above method the eigenfunctions Ψ_n were calculated in a two-dimensional grid with 80 × 100 elements. Examples of computed shapes of Ψ_n are plotted in Fig. 2 in the form of filled contour maps which are a two-dimensional representation of three-dimensional data. In these plots contours define lines of constant value of Ψ_n. The computed eigenfunctions Ψ_n represent the numerical solution of the wave equation in a two-dimensional area in the shape of the room's horizontal cross-section satisfying the Neumann boundary condition. The results depicted in Fig. 2 imply that for some eigenmodes the acoustic energy can be concentrated inside the one of subrooms (Figs. 2a,d). This effect, often called mode localization, is characteristic for fractal structures [27] and enclosures having an irregular geometry [28].

3.2 Steady-state sound pressure

In steady-state the spatial distribution of the RMS pressure P inside a room can be predicted from Eq. (9) using the computed eigenfunctions Ψ_n and eigenfrequencies ω_n. Calculations of P were carried out in the observation plane $z = 1.8$ and a sound source placed in two points: $x_0 = 2$, $y_0 = 5$, $z_0 = 1$ and $x_0 = 8$, $y_0 = 5$, $z_0 = 1$ (all dimensions in meters). The first point is located in the subroom A whereas the second one in the subroom B. In a numerical simulation the first 140 eigenmodes, having eigenfrequencies from the range 0–170 Hz, were used. For a sake of model simplicity the wall impedance was assumed to be purely real, i.e. the mass and stiffness of the absorbing material are neglected. This corresponds to the damping of a sound wave on the wall with no phase change upon reflection.

In order to examine the influence of sound absorption on the distribution of the pressure P, it was assumed that the values of the random incidence absorption coefficient[†] of the walls in subrooms A and B were selected in such a way that the average absorption coefficient $\overline{\alpha}$ in a room remains constant, thus

$$\overline{\alpha} = \frac{\alpha_a S_a + \alpha_b S_b + \alpha_{ab} S_{ab}}{S} = \text{const.}, \tag{17}$$

[†] Also known as random-absorption coefficient [26] or statistical absorption coefficient [29].

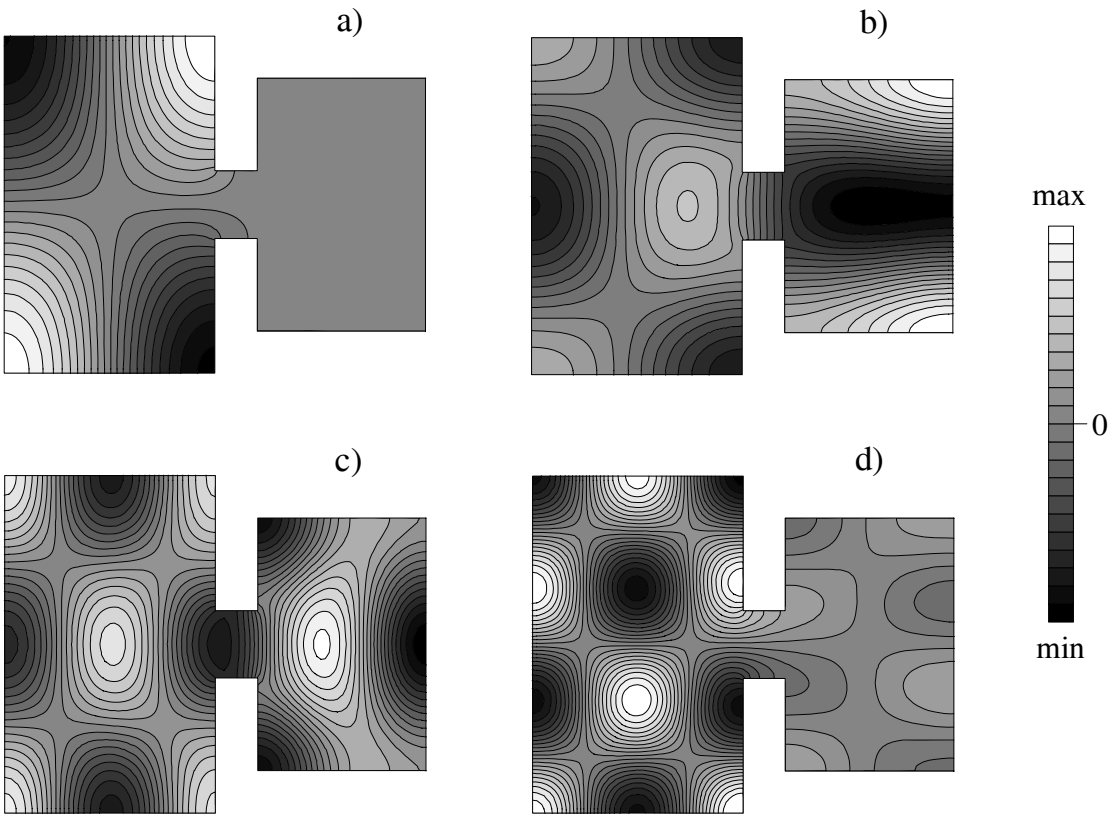

Fig. 2 Shapes of functions Ψ_n for mode numbers: a) $n = 5$, b) $n = 10$, c) $n = 15$, d) $n = 20$.

where α_a and S_a are the absorption coefficient and the surface area of the walls in the subroom A, α_b and S_b are the absorption coefficient and the surface area of the walls in the subroom B, α_{ab} and S_{ab} are the absorption coefficient and the surface area of the walls in the part of the room connecting subrooms A and B, respectively, and $S = S_a + S_{ab} + S_b$. For a given value of the coefficient $\overline{\alpha}$, the surface impedances on room walls were found from the well-known relationship between the random incidence absorption coefficient α and the impedance ratio ξ [25]

$$\alpha = \frac{8}{\xi}\left[1 + \frac{1}{1+\xi} - \frac{2}{\xi}\ln(1+\xi)\right], \quad \xi = Z/\rho c. \tag{18}$$

In the calculation procedure it was assumed that $\overline{\alpha} = \alpha_{ab} = 0.15$, thus the coefficients α_a and α_b in subrooms A and B were changing quantities. It is important to note that the assumed value of the coefficient $\overline{\alpha}$ is close to the average absorption coefficients of slightly vibrating walls (a suspended ceiling for example) or moderately absorbing surfaces (a painted concrete block) in the octave band with a centre frequency of 125 Hz (usually, the lowest octave band in tables of material absorption coefficients) [1].

The plots in Fig. 3 depict examples of the calculated RMS pressure P obtained for two distributions of absorbing material on the room walls and different frequencies and locations of the sound source. These data imply that for a large difference between

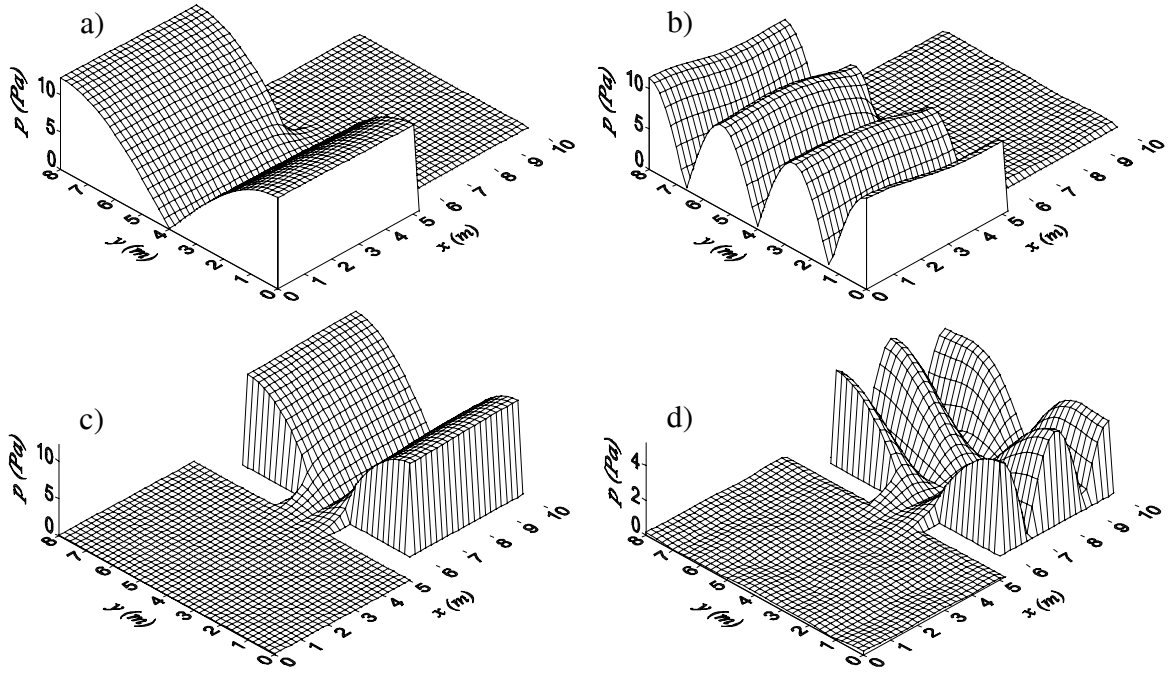

Fig. 3 Distributions of RMS pressure for two configurations of absorbing material and different frequencies and positions of sound source: (a,b) $\alpha_a = 0.015$, $\alpha_b = 0.35$, 21.7 Hz and 64.7 Hz, source in subroom A, (c,d) $\alpha_a = 0.24$, $\alpha_b = 0.016$, 29.1 Hz and 90.5 Hz, source in subroom B.

absorption coefficients α_a and α_b at some frequencies there is a substantial difference between the values of the pressure P in both subrooms. In order to investigate this effect in more detail, from the distribution of P in an observation plane the average value $\overline{P}$ in subrooms A and B was computed for an assumed driving frequency f and a location of the sound source. A frequency dependence of $\overline{P}$ calculated for various values of the absorption coefficients α_a and α_b are shown in Fig. 4. The data presented in Figs. 4a,b,c were obtained for $\alpha_a \leq \alpha_b$ and the sound source located in the subroom A. As may be seen, for subroom walls covered by the same absorbing material ($\alpha_a = \alpha_b$) there are very small differences of $\overline{P}$ inside subrooms A and B (Fig. 4c). Although the total room absorption was assumed to be a constant parameter, a decrease in the ratio α_a/α_b results in a very interesting behaviour of the frequency dependence of $\overline{P}$, namely: very small changes in $\overline{P}$ in subroom B (solid lines) are accompanied with a substantial increase in $\overline{P}$ in subroom A for some sound frequencies (dashed lines), and moreover, when the ratio α_a/α_b decreases the peaks of $\overline{P}$ in the subroom A are visibly higher (Figs. 4a,b). A very similar phenomenon is observed if $\alpha_a \geq \alpha_b$ and a sound source is located in the subroom B (Figs. 4d,e,f). However in this case one can notice an influence of a relation between the absorption coefficients α_a and α_b on the sound pressure inside the subroom B. Furthermore, contrary to the situation shown in Figs. 4a,b distinct peaks in the frequency dependence of $\overline{P}$ appear when the sound absorption in subroom B is much smaller than in subroom A (Fig. 4d). Also, the total amount of peaks in the assumed range of f and

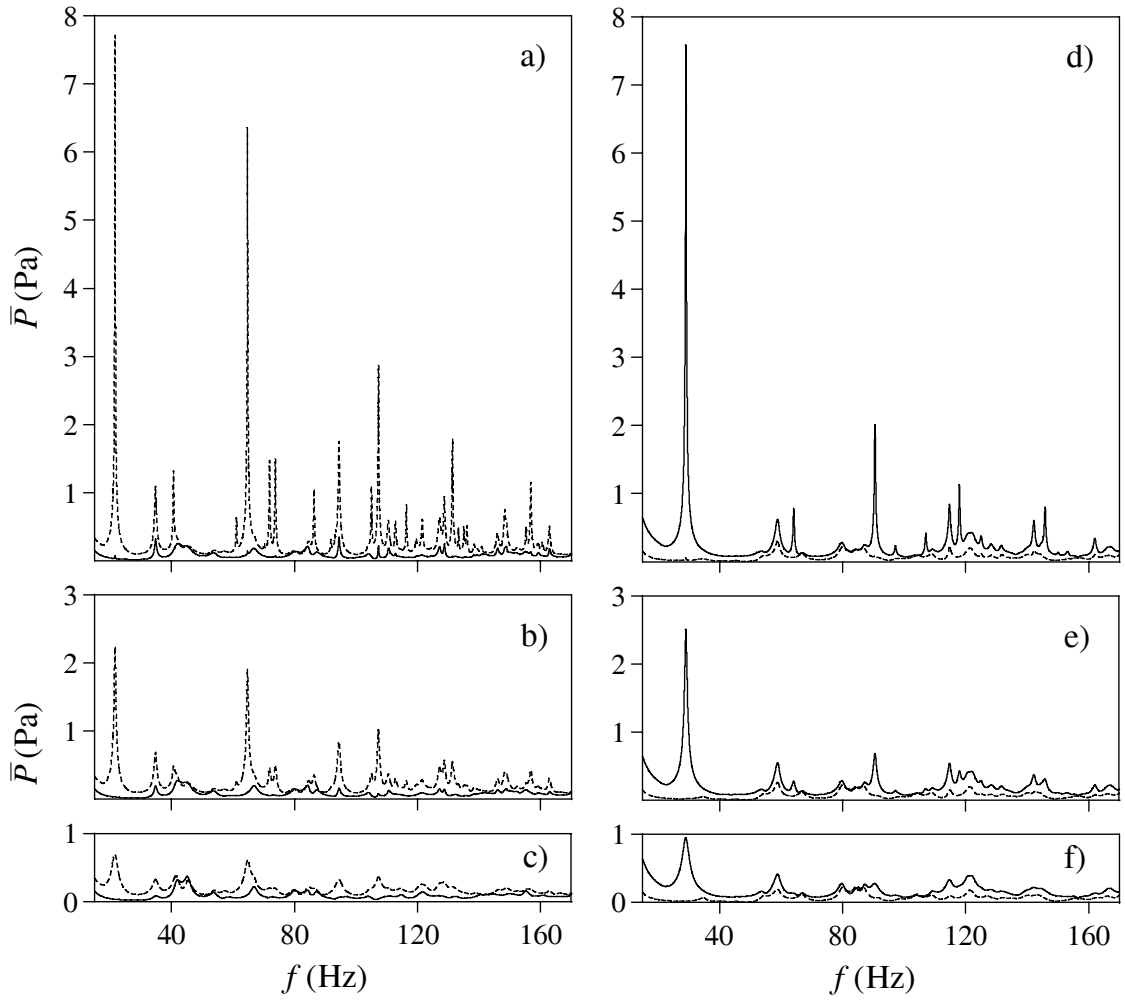

Fig. 4 Frequency dependence of average value of the RMS pressure in subroom A (dashed lines) and subroom B (solid lines) for a sound source located in subroom A (a,b,c) and subroom B (d,e,f) for different distributions of absorbing material on room walls: (a) $\alpha_a = 0.015$, $\alpha_b = 0.35$, (b) $\alpha_a = 0.05$, $\alpha_b = 0.3$, (c,f) $\alpha_a = \alpha_b = 0.15$, (d) $\alpha_a = 0.24$, $\alpha_b = 0.016$, (e) $\alpha_a = 0.21$, $\alpha_b = 0.06$.

their frequencies is different in both cases.

The appearance of narrow peaks in the frequency dependence of $\overline{P}$ occurring for large differences between coefficients α_a and α_b indicates that the pressure distribution inside the room is influenced by mode localization and it can be explained as follows. Suppose that the sound frequency is close to an eigenfrequency of the mode (m, n) which is localized in the subroom A, for instance. This means that the acoustic energy associated with this mode is concentrated in the subroom A, so in consequence the highest values of the eigenfunction Ψ_n squared occur in this subroom and values of Ψ_n^2 are very small in the remaining part of the room (Figs. 2a,d). Because of this property a sound emitted by a harmonic source having a frequency of this eigenmode is mainly absorbed in this subroom and weakly damped in the subroom B. Thus, it is clear that in this case the

pressure $\overline{P}$ in the subroom A peaks strongly when the condition $\alpha_a \ll \alpha_b$ is satisfied.

The frequencies of localized modes can be found from the distribution of eigenfunctions Ψ_n in (x, y) plane. Since they are normalized over a room's horizontal cross-section, the integral $\int_\sigma \Psi_n^2 \mathrm{d}x\mathrm{d}y$ equals unity then to characterize mathematically the localization or the confinement of eigenmodes one should compute two non-dimensional parameters

$$\upsilon_n^a = \int_{\sigma_a} \Psi_n^2 \mathrm{d}x\mathrm{d}y, \qquad \upsilon_n^b = \int_{\sigma_b} \Psi_n^2 \mathrm{d}x\mathrm{d}y, \tag{19a,b}$$

where σ_a and σ_b are surfaces of horizontal cross-sections of subrooms A and B. Thus, an eigenmode is localized in subroom A when the parameter υ_n^a is very close to unity or a value of υ_n^b is very small. Dependencies of the parameters υ_n^a (circles) and υ_n^b (triangles) on the sound frequency f are depicted in Fig. 5. Calculation results indicate that for some

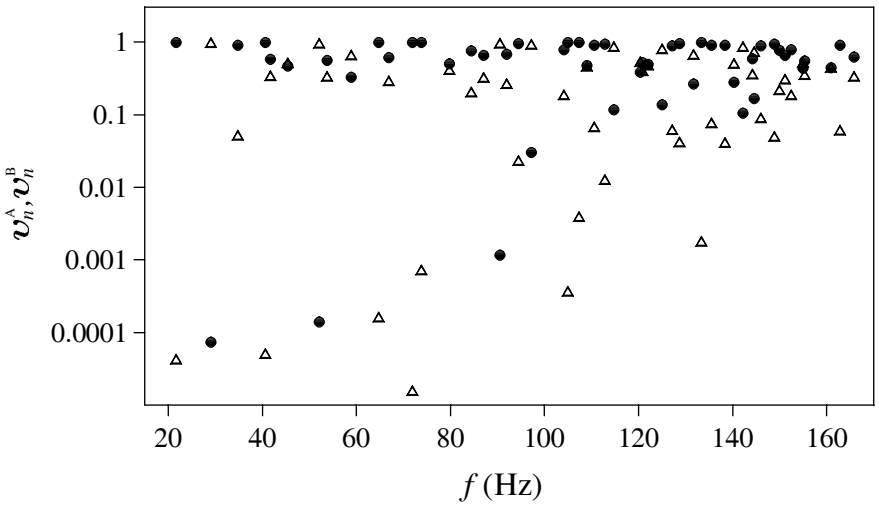

Fig. 5 Non-dimensional parameters υ_n^a (circles) and υ_n^b (triangles) versus sound frequency.

modes, which can be termed as strongly localized modes, the parameters υ_n^a and υ_n^b have values smaller than 0.01. The frequencies of these modes are presented in Table 1, where in the main and bottom parts are collected eigenmodes localized in subrooms A and B, respectively. As follows from a comparison between Fig. 4a,d and the data in the second column of Table 1, frequencies of the strongly localized modes correspond to frequencies at which the average value of RMS pressure inside the subrooms A and B peaks. To recognize the cause of mode localization, the eigenfrequencies $f_{\kappa\nu}$ of a rectangle

$$f_{\kappa\nu} = \frac{c}{2\pi}\sqrt{\left(\frac{\kappa\pi}{d}\right)^2 + \left(\frac{\nu\pi}{l}\right)^2} \tag{20}$$

with dimensions d and l corresponding to the dimensions of cross-sectional areas of the subrooms were computed, where $\kappa, \nu = 0, 1, 2...$ and $d = d_1$, $l = l_1$ for subroom A and $d = d_4$, $l = l_3$ for subroom B (Fig. 1). In Table 1 some frequencies $f_{\kappa\nu}$ are listed, together with the corresponding combinations of subscripts κ and ν. These data indicate that the effect of mode localization in the room consisting of two connected rectangular subrooms

is caused by a generation of eigenmodes having approximately the same frequency as eigenmodes in rectangular enclosures with the same dimensions as the subrooms.

Table 1 Frequencies f_n of eigenmodes strongly localized in subroom A (upper part of table) and subroom B (bottom part of table) in comparison with frequencies $f_{\kappa\nu}$ calculated from Eq. (20).

n	f_n (Hz)	κ	ν	$f_{\kappa\nu}$ (Hz)
2	21.670	0	1	21.438
5	40.684	1	1	40.448
11	64.726	0	3	64.313
13	71.896	2	1	71.872
14	73.787	1	3	72.888
23	105.018	3	1	105.109
24	107.311	0	5	107.187
36	133.323	1	6	133.120
3	29.083	0	1	28.583
8	52.061	1	1	51.529
18	90.538	2	1	90.388

3.3 Reverberant sound decay

For given source parameters (the frequency, the distribution) and an assumed configuration of absorbing material on the subrooms' walls a formula obtained by inserting expressions (10a,b) into Eq. (1) makes it possible to predict the reverberation time at each point of the room space from the calculated energy decay curves corresponding to the time history of the sound pressure level

$$L = 20\log(|p|/p_0), \tag{21}$$

where p_0 is a reference pressure. Since the functions P_{mn} in Eq. (10b) include harmonic terms, from temporal changes in the pressure level L a time-average decay curve was calculated using the method of a polynomial regression. A fitted curve obtained in such a way describes the average long-time changes in the sound pressure level, thus it was applied to determine the standard reverberation time T which is defined as the time for the sound to die away to a level 60 decibels below its original level. Examples of pressure level decay curves together with fitting curves calculated at two observation points for a source located in subroom A and the sound frequency corresponding to an eigenfrequency of a mode localized in subroom B are presented in Fig. 6. Plots in this figure exhibit various slope characteristics of decay curves. In the first case, shown in Fig. 6a, the time-average decay of pressure level is linearly dependent on the time, which means that that sound pressure has an exponential decay. This situation occurs when the pressure level decay is dominated by a decay of one eigenmode or by decays of eigenmodes having the same or very similar damping coefficients. Plots presented in Fig. 6b depict a reverberant process for a large difference between the absorption coefficients α_a and α_b.

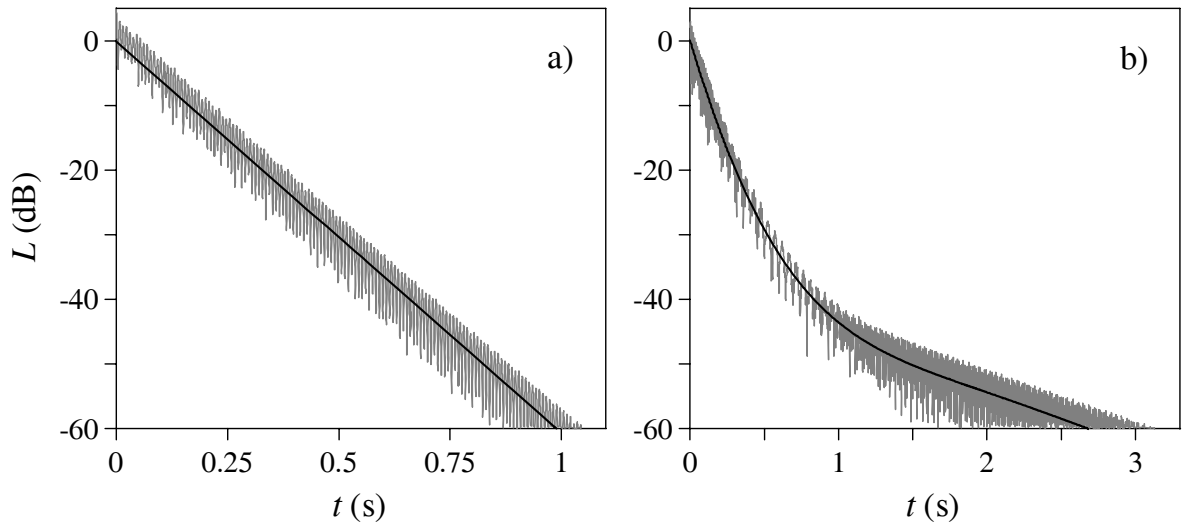

Fig. 6 Pressure level decay curves (gray lines) and fitting curves (solid black lines) obtained using the method of polynomial regression for a frequency of 52.1 Hz corresponding to an eigenfrequency of a mode localized in subroom B for two different distributions of absorbing material on subrooms walls: (a) $\alpha_a = \alpha_b = 0.15$, observation point in subroom A: $x = 4$ m, $y = 2$ m, $z = 1.8$ m, (b) $\alpha_a = 0.24$, $\alpha_b = 0.016$, observation point in subroom B: $x = 8$ m, $y = 2$ m, $z = 1.8$ m. Sound source located in subroom A.

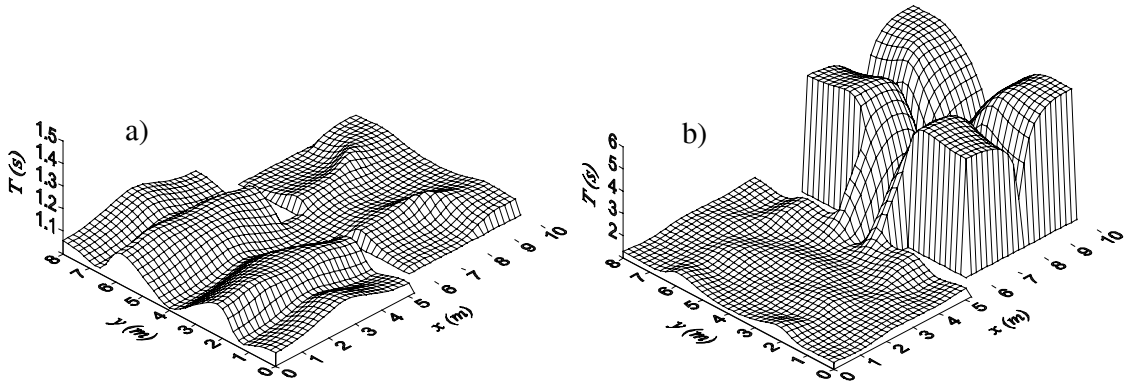

Fig. 7 Distributions of the reverberation time for a frequency of 52.1 Hz corresponding to an eigenfrequency of a mode localized in subroom B for two configurations of absorbing material on subrooms walls: (a) $\alpha_a = \alpha_b = 0.15$, (b) $\alpha_a = 0.24$, $\alpha_b = 0.016$. Sound source located in subroom A.

In this case the decay curve consists of two parts which refer to the rapid early decay and the slow late decay, thus it can be well approximated by polynomial function of higher degree (degree 8 in this case). In such a situation the time history of a pressure level characterises a double-sloped effect (DSE), which happens when a dominant acoustic mode is much more damped than neighbouring modes. In the case shown in Fig. 6b, a rapid early sound decay may result in higher sound clarity, whereas a slow late decay

leads to an increase in perceived reverberance. Thus, from a subjective viewpoint the standard reverberation appears to be a somewhat misleading measure of DSE. In the past different metrics were proposed to quantify DSE. Harrison and Madaras [30] characterized a coupled rooms' effect by the ratio T_{30}/T_{15}, referred to as the "coupling coefficient", where T_{30} is given as the decay time from -5 to -35 dB in the decay curve, multiplied by a factor of 2, whereas T_{15} is defined as the decay time from -5 to -20 dB, multiplied by a factor of 4. In a study of sound decay in coupled-volume concert halls Ermann and Johnson [31] used the ratio T/T_{15}, referred to as the "coupling constant", which is a slight modification on the coupling coefficient. Both metrics are not unequivocal measures of DSE, because different sound decay curves are capable of producing the same coupling coefficient or coupling constant. In order to characterize different double-sloped profiles accurately, Bradley and Wang [13] used two quantities: the decay ratio T_2/T_1 and the parameter Δ, where T_1 and T_2 are the early and late reverberation times and Δ is found from a linear approximation of the late decay curve. As was shown in the Appendix, in the room under consideration participation of neighbouring eigenmodes in producing the sound decay varies from point to point giving decay curves which can be described by different values of T_1, T_2 and Δ. Thus, by use of these metrics it is difficult to quantify a sound reverberation process in each of the subrooms. For this reason the standard reverberation time T, treated more like a physical measure than a metric of DSE, will be utilized to characterize a reverberation phenomenon in the room system being analyzed.

Figure 7 shows examples of distributions of the reverberation time T computed in an observation plane for previously assumed source parameters and configurations of absorbing material on room walls. As may be seen, for the uniform distribution of absorbing material the reverberation time T varies very slightly (Fig. 7a). However, when the absorption coefficient α_b is much smaller than α_a large values of the reverberation time T in the subroom B are observed for a sound frequency equal to an eigenfrequency of a mode strongly localized in the subroom B (Fig. 7b). In order to investigate this effect in the whole frequency range, from the distribution of T in an observation plane the average value $\overline{T}$ of the reverberation time in subrooms A and B was computed. Frequency dependencies of $\overline{T}$ for assumed source locations and different distributions of absorbing material on the subrooms' walls are shown in Fig. 8.

The graphs presented are of great importance from a practical viewpoint because they show how the distribution of absorbing material on room walls can strongly influence the decay of the sound pressure inside the subrooms. As follows from Fig. 8, if a difference between the absorption coefficients in the subrooms is sufficiently high a great increase in the average reverberation time $\overline{T}$ is observed for some sound frequencies. A detailed analysis of the calculation data has proved that local maxima of the time $\overline{T}$ occur for frequencies of modes which are localized in such a subroom where a sound damping is smaller. It is important to note that this effect is the direct result of an irregular geometry of lateral walls in the room under consideration because in a rectangular room all eigenmodes are delocalized [27].

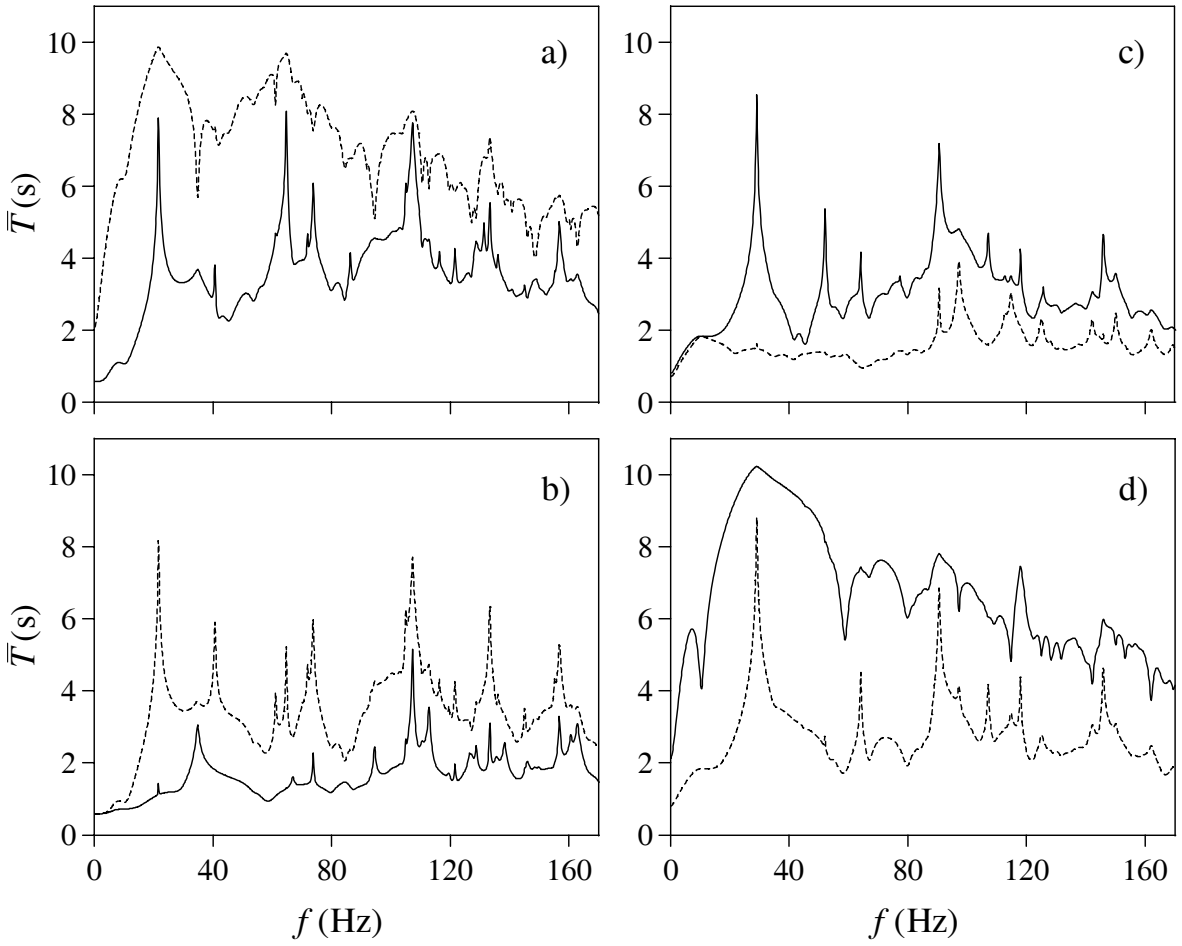

Fig. 8 Frequency dependence of the average value of the reverberation time in subroom A (dashed lines) and subroom B (solid lines) for a sound source located in subroom A (a,c) and subroom B (b,d) for two distributions of absorbing material on room walls: (a,b) $\alpha_a = 0.015$, $\alpha_b = 0.35$, (c,d) $\alpha_a = 0.24$, $\alpha_b = 0.016$.

As may be seen in Fig. 8, the frequency dependence of the reverberation time is also influenced by the position of the source. When it is located in a subroom whose walls are covered by a material with a large absorption, sharp high-valued peaks of the reverberation time $\overline{T}$ are only observed in the coupled subroom because of the small damping of acoustic energy for localized eigenmodes (Fig. 8b,c). On the other hand, if the sound source position is in a subroom with small sound damping, typical narrow peaks of reverberation time occur in the second subroom as before (Fig. 8a,d), however in the frequency dependence of $\overline{T}$ in the first subroom the reverberation time is high but there are not sharp peaks. This may be explained by the fact that a mode localized in this subroom has a high amplitude in a steady-state (Fig. 4a,d), thus it dominates the reverberant energy decay in a wide frequency range.

4 Conclusions

In the low frequency range a method of eigenmodes has been used for studying the acoustic parameters of a lightly damped, irregularly shaped room consisting of two connected rectangular subrooms. The effects of acoustical coupling between the subrooms on steady-state and reverberant sound fields have been investigated for different distributions of absorbing materials on the subrooms' walls under the assumption that the total room absorption was constant.

Results of a numerical simulation have shown that the location of absorbing material and the position of the sound source have a great influence on the distribution of the sound pressure and the reverberation time inside the subrooms. It was found that this is the result of the modal localization which appears in enclosures of irregular geometry such as the system of coupled subrooms that was analyzed. For a large difference between the absorption properties of the subrooms this effect entails an unwanted, substantial increase in the sound pressure and the reverberation time for frequencies of strongly localized eigenmodes. A detailed analysis of the numerical data has shown that in the room under consideration the effect of mode localization is caused by the generation of eigenmodes having approximately the same frequency as eigenmodes in rectangular enclosures with the same dimensions as the subrooms.

It was found that for a large difference between the absorption properties of subrooms the time history of the sound pressure exhibits an interaction of modes in producing a decay curve from which the reverberation time is evaluated. In such a situation there is a possibility for an interesting effect to occur, namely reverberant curves that exhibit double-sloped decay. In this case the pressure level change is rapid initially and much slower during the late stage of the sound decay. This is result of different damping coefficients for eigenmodes having comparable eigenfrequencies and it appears when a dominant mode is much more damped than neighbouring modes.

Appendix

Characteristics of double-sloped decay

According to a general classification of different shapes of non-exponential sound decay [32], the decay curve shown in Fig. 6b exhibits a "sagging" appearance with a clearly visible rapid initial decay and a shallow late decay slope. To quantify the sag of the double-sloped decay the initial and late damping factors can be found via approximating the decay curve by a function including a combination of two exponential decays

$$F(t) = 20 \log \left[\frac{1}{1+A} \left(e^{-r_1 t} + A e^{-r_2 t} \right) \right], \tag{A1}$$

which satisfies the condition $F(0) = 1$, where r_1 and r_2 are the damping factors for initial and late portions of sound decay, respectively, and A is the ratio between the amplitudes

of the late and the initial decays. A comparison between the decay curve (solid line) and the fitting curve (dashed line) is depicted in Fig. 9a.

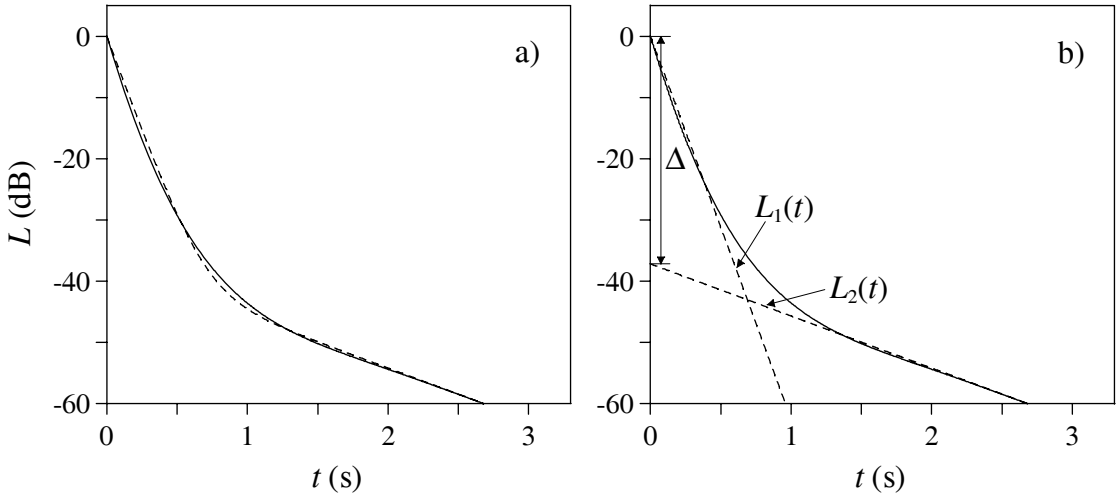

Fig. 9 Approximation of the decay curve from Fig. 6b (solid line) by: (a) function (A1) including the sum of two exponential decays (dashed line), (b) modal decay equations (A3) for $T_1 = 0.958$ s, $T_2 = 7.063$ s and $\Delta = 37.2$ dB (dashed lines).

The best approximation was obtained for the following parameters: $r_1 = 7.21\ \mathrm{s}^{-1}$, $r_2 = 0.978\ \mathrm{s}^{-1}$ and $A = 1.402 \cdot 10^{-2}$. Now, using the estimated damping factors and the formula for the modal reverberation time [26]

$$T_m = 3\ln(10)/r, \tag{A2}$$

it is easy to compute the reverberation times T_1 and T_2 for early and late sound decays, respectively. However, these times are insufficient metrics to definitively identify a double-sloped decay because the sag of this decay can be different for the same times T_1 and T_2. Thus, as was shown by Bradley and Wang [13] a third parameter — Δ — should be defined to characterize a double-sloped profile of sound decay. This parameter is present in the modal decay equations

$$L_1(t) = -\left(\frac{60}{T_1}\right)t, \qquad L_2(t) = -\left(\frac{60}{T_2}\right)t - \Delta, \tag{A3}$$

approximating the decays of pressure level in the early and the late stages of a reverberant process by straight lines (Fig. 9b). The use of the second equation together with a calculated value of the reverberation time T_2 enables the best estimate of Δ to be found. Figure 9b indicates that for initial and late decays of the pressure level that may be well approximated by the modal decay equations (A3), the quantities T_1, T_2 and Δ seem to be the appropriate characteristics of a double-sloped decay.

In the case of the room that was analyzed participation of neighbouring eigenmodes in producing the sound decay varies from point to point, giving decay profiles which can be characterized by different values of the parameters T_1, T_2 and Δ. It is particularly

visible for large differences between the absorption coefficients α_a and α_b and for a sound frequency equal to an eigenfrequency of a strongly localized mode. Examples of decay curves obtained in this case are shown in Fig. 10.

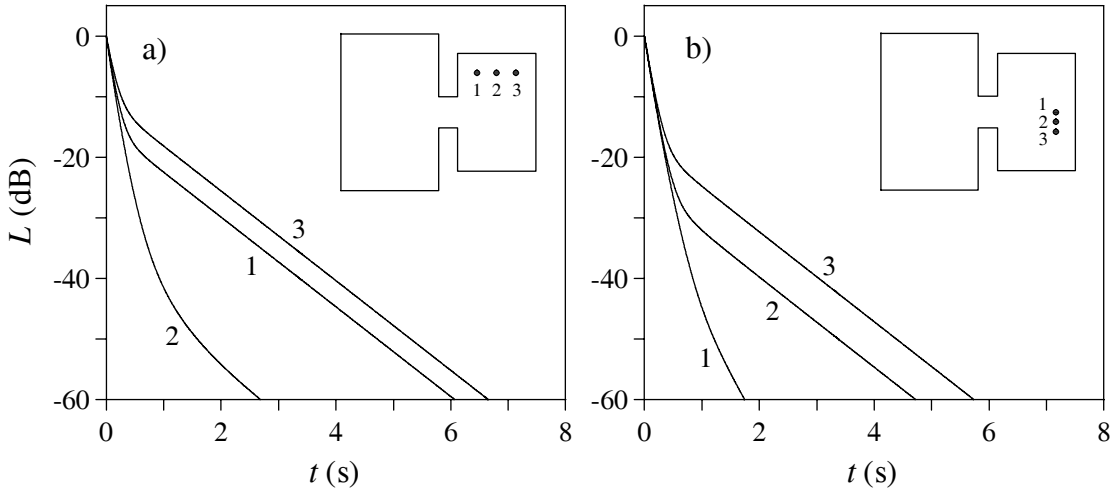

Fig. 10 Calculated sound decay curves in points 1, 2 and 3 in the observation plane z = 1.8 m (black points in room horizontal-cross section) for absorption coefficients α_a = 0.24, α_b = 0.016 and sound frequency of 52.1 Hz. Sound source located in subroom A.

As may be seen, at some observation points the early decay is very short and a reverberation process is dominated by the late decay with a shallow slope (curves 1 and 3 in Fig. 10a, curves 2 and 3 in Fig. 10b). This leads to a high value of standard reverberation time and corresponds to a small value of the parameter Δ. The remaining two decay curves (curve 2 in Fig. 10a, curve 1 in Fig. 10b) prove, however, that this parameter may change very rapidly from point to point. For all curves in Fig. 10 and curves 2 and 3 in Fig. 10b the late portion of the sound decay may by approximated by straight lines with similar slopes giving comparable values of the late reverberation time T_2 (curve 1 in Fig. 10b characterizes an evidently various late decay slope). However, this property is not observed in the initial portion of decay curves showing that in these cases the early reverberation time T_1 is somewhat different.

References

[1] H. Kuttruff: *Room acoustics*, Applied Science Publishers, London, 1973.
[2] P.M. Morse and R.H. Bolt: "Sound waves in rooms", *Rev. Mod. Phys.*, Vol. 16, (1994), pp. 69–150.
[3] M. Heckl: *Reverberation. Modern Methods in Analytical Acoustics*, Springer-Verlag, New York, 1992.
[4] P.M. Morse and K.U. Ingard: *Theoretical acoustics*, Mc Graw-Hill, New York, 1968.

[5] E.H. Dowell, G.F. Gorman III and D.A. Smith: "Acoustoelasticity: general theory, acoustic natural modes and forced response to sinusoidal excitation, including comparison to experiment", *J. Sound Vib.*, Vol. 52, (1977), pp. 519–542.
[6] C.F. Eyring: "Reverberation time measurements in coupled rooms", *J. Acoust. Soc. Amer.*, Vol. 2, (1931), pp. 181–206.
[7] C.M. Harris and H. Feshbach: "On the acoustics of coupled rooms", *J. Acoust. Soc. Amer.*, Vol. 22, (1950), pp. 572–578.
[8] L. Cremer and H.A. Müller: *Principles and applications of room acoustics*, Applied Science, London, 1978.
[9] C. Thompson: "On the acoustics of a coupled space", *J. Acoust. Soc. Amer.*, Vol. 75, (1984), pp. 707–714.
[10] R.L. Weaver and O.I. Lobkis: "Anderson localization in coupled reverberation rooms", *J. Sound Vib.*, Vol. 231, (2000), pp. 1111–1134.
[11] J.S. Anderson, M. Bratos-Anderson and P. Donay: "The acoustics of a large space with a repetitive pattern of coupled rooms", *J. Sound Vib.*, Vol. 208, (1997), pp. 313–329.
[12] J.S. Anderson and M. Bratos-Anderson: "Acoustic coupling effects in St Paul's Cathedral, London", *J. Sound Vib.*, Vol. 236, (2000), pp. 209–225.
[13] D.T. Bradley and L.M. Wang: "The effects of simple coupled volume geometry on the objective and subjective results from nonexponential decay", *J. Acoust. Soc. Amer.*, Vol. 118, (2005), pp. 1480–1490.
[14] J.E. Summers, R.R. Torres, Y. Shimizu and B.L. Dalenbäck: "Adapting a randomized beam-axis-tracing algorithm to modeling of coupled rooms via late-part ray tracing", *J. Acoust. Soc. Amer.*, Vol. 118, (2005), pp. 1491–1502.
[15] J.E. Summers, R.R. Torres and Y. Shimizu: "Statistical-acoustics models of energy decay in systems of coupled rooms and their relation to geometrical acoustics", *J. Acoust. Soc. Amer.*, Vol. 116, (2004), pp. 958–969.
[16] A. Billon, V. Valeau, A. Sakout and J. Picaut: "On the use of a diffusion model for acoustically coupled rooms", *J. Acoust. Soc. Amer.*, Vol. 120, (2006), pp. 2043–2054.
[17] O.C. Zienkiewicz: *The finite element method in engineering sciences*, Mc Graw-Hill, London, 1977.
[18] V. Easwaran and A. Craggs: "On futher validation and use of the finite element method to room acoustics", *J. Sound Vib.*, Vol. 187, (1995), pp. 195–212.
[19] C.A. Brebbia, J.C.F. Telles and L.C. Wrobel: *Boundary element techniques*, Springer, New York, 1984.
[20] Y. Hobiki, K. Yakubo and T. Nakayama: "Spectral characteristics in resonators with fractal boundaries", *Phys. Rev. E*, Vol. 54, (1996), pp. 1997–2004.
[21] B. Sapoval and Th. Gobron: "Vibrations of strongly irregular or fractal resonators", *Phys. Rev. E*, Vol. 47, (1993), pp. 3013–3024.
[22] B. Sapoval, O. Haeberlé and S. Russ: "Acoustical properties of irregular and fractal cavities", *J. Acoust. Soc. Amer.*, Vol. 102, (1997), pp. 2014–2019.

[23] S.W. Kang and J.M. Lee: "Eigenmode analysis of arbitrarily shaped two-dimensional cavities by the method of point-matching", *J. Acoust. Soc. Amer.*, Vol. 107, (2000), pp. 1153–1160.

[24] M. Meissner: "Influence of wall absorption on low-frequency dependence of reverberation time in room of irregular shape", accepted for publication in *Appl. Acoust.*.

[25] L.E. Kinsler and A.R. Frey: *Fundamentals of acoustics*, John Wiley & Sons, New York, 1962.

[26] E.H. Dowell: "Reverberation time, absorption, and impedance", *J. Acoust. Soc. Amer.*, Vol. 64, (1978), pp. 181–191.

[27] S.Russ, B. Sapoval and O. Haeberlé: "Irregular and fractal resonators with Neumann boundary conditions: density of states and localization", *Phys. Rev. E*, Vol. 55, (1997), pp. 1413–1421.

[28] M. Meissner: "Influence of room geometry on low-frequency modal density, spatial distribution of modes and their damping", *Arch. Acoust.*, Vol. 30 (Supplement), (2005), pp. 203–208.

[29] K.S. Sum: "Some comments on Sabine absorption coefficient", *J. Acoust. Soc. Amer.*, Vol. 117, (2005), pp. 486–489.

[30] B. Harrison and G. Madaras: "Computer modeling and prediction in the design of coupled volumes for a 1000-seat concert hall at Goshen College, Indiana", *141st Meeting of the Acoustical Society of America, J. Acoust. Soc. Amer.*, Vol. 109, (2001), p. 2388.

[31] M. Ermann and M. Johnson: "Pilot study: Exposure and materiality of the secondary room and its impact on the impulse response of coupled-volume concert halls", *143st Meeting of the Acoustical Society of America, J. Acoust. Soc. Amer.*, Vol. 111, (2002), p. 2331.

[32] M. Barron: "Interpretation of early decay times in concert auditoria", *Acustica*, Vol. 81, (1995), pp. 320–331.